

# Placement and Design of SVC Device For Voltage Stability Studies

O. L. BEKRI, M.K. FELLAH, and M. F. BENKHORIS

**Abstract**— one of the major causes of voltage (load) instability is the reactive power limit of the system. Improving the system's reactive power handling capacity via a Flexible AC transmission system (FACTS) devices is a remedy for prevention of voltage instability and hence voltage collapse. In this paper, a methodology for optimal locating the Static Var Compensator (SVC) in order to enhance the static voltage stability margin is presented. For ensure the robustness of the proposed method and gives a practical sense of our study, N-1 contingency analysis of power system is considered.

Based on results at the point of collapse, design strategies are proposed for this device, so that its location dimensions can be optimally defined to increase system loadability. The IEEE14 bus test system is used to illustrate the application of SVC model and techniques.

**Index Terms**— FACTS, SVC, CPFlow, Voltage Stability, N-1 contingency analysis

## I. INTRODUCTION

IN recent years, the increase in peak load demand and power transfers between utilities has elevated concerns about system voltage security.

Voltage stability can also called "load stability" [1]. Voltage stability is a problem in power systems which are heavily loaded, faulted or have a shortage of reactive power. The nature of voltage stability can be analysed by examining the production, transmission and consumption of reactive power. The problem of voltage stability concerns the whole power system, although is usually has a large involvement in one critical area of the power system.

The main factor causing voltage instability is the inability of the power system to meet the demands for reactive power in the heavily stressed systems to keep desired voltages. The loadability of a bus in the power system depends on the reactive power support that the bus can receive from the system.

As the system approaches the maximum loading point or voltage collapse point, both real and reactive power losses increase rapidly. Therefore, the reactive power supports have to be local and adequate.

There are two types of voltage stability based on the time frame of simulation: static voltage stability and dynamic

voltage stability. Static analysis involves only the solution of algebraic equations and therefore is computationally less extensive than dynamic analysis.

Static voltage stability is ideal for the bulk of studies in which voltage stability limit for many pre-contingency and post-contingency cases must be determined.

In static voltage stability, slowly developing changes in the power system occur that eventually lead to a shortage of reactive power and declining voltage.

This phenomenon can be seen from the plot of the power transferred versus the voltage at receiving end. The plots are popularly referred to as P-V curve or "Nose" curve. As the power transfer increases, the voltage at the receiving end decreases. Eventually, the critical (nose) point, the point at which the system reactive power is short in supply, is reached where any further increase in active power transfer will lead to very rapid decrease in voltage magnitude. Before reaching the critical point, the large voltage drop due to heavy reactive power losses can be observed.

The only way to save the system from voltage collapse is to reduce the reactive power load or add additional reactive power prior to reaching the point of voltage collapse [2].

Voltage collapse phenomena in power systems have become one of the important concerns in the power industry over the last two decades, as this has been the major reason for several major blackouts that have occurred throughout the world including the recent Northeast Power outage in North America in August 2003 [3]. Point of collapse method and continuation method are used for voltage collapse studies [4].

Of these two techniques continuation power flow method is used for voltage analysis. These techniques involve the identification of the system equilibrium points or voltage collapse points where the related power flow Jacobian becomes singular [5, 6].

The flexible AC transmission system (FACTS) has received much attention in the last 2 decades. It uses high current power electronic devices to control the voltage, power flow, stability, etc. of a transmission system. FACTS devices can be connected to a transmission line in various ways, such as in series, shunt, or a combination of series and shunt. For example, the static VAR compensator (SVC) and static synchronous compensator (STATCOM) are connected in shunt; static synchronous series compensator (SSSC) and thyristor controlled series capacitor (TCSC) are connected in series; thyristor controlled phase shifting transformer (TCPST)

and unified power flow controller (UPFC) are connected in a series and shunt combination.

Canizares and Faur studied the effects of SVC and TCSC on voltage collapse [7]. Study of STATCOM and UPFC Controllers for Voltage Stability Evaluated by Saddle-Node Bifurcation Analysis is carry out in [8].

In this paper, a methodology, based on a continuation power flow analysis (CPF), is used to evaluate the effects of the SVC device on the system maximum loading point in voltage stability study. Utilization of SVC during single contingencies is investigated. The continuous power flow analysis consists of a predictor step realised by the computation of the tangent vector and a corrector step that can be obtained either by means of a local parameterization or a perpendicular intersection.

The rest of the paper is organized as follows: Section II introduces the basic mathematical tools required for the analysis of voltage collapse phenomena. Continuation power flow analysis is presented in section III. FACTS modeling is presented in section IV.

In section V, some interesting results are presented along with detailed discussion finally; our contributions and conclusions are summarized in Section VI.

## II. VOLTAGE COLLAPSE

Voltage collapse studies and their related tools are typically based on the following general mathematical description of the system [9]:

$$\begin{aligned} \dot{x} &= f(\dot{x}, y, \lambda, p) \\ 0 &= g(x, y, \lambda, p) \end{aligned} \quad (1)$$

where

$x \in \mathcal{R}^n$  Represents the system state variables, corresponding to dynamical states of generators, loads, and any other time varying element in the system, such as FACTS controllers;

$y \in \mathcal{R}^n$  Corresponds to the algebraic variables, usually associated to the transmission system and steady-state element models, such as some generating sources and loads in the network.

$\lambda \in \mathcal{R}^k$  Stand for a set of uncontrolled parameters that drive the system to collapse, which are typically used to system demand.

Vector  $p \in \mathcal{R}^k$  is used here to represent system parameters that are directly controllable, such as shunt and series compensation levels.

Based on (1), the collapse point may be defined, under certain assumptions, as the equilibrium point where the related

system Jacobian is singular, i.e., the point  $(x_0, y_0, \lambda_0, p_0)$  where

$$\begin{bmatrix} f(x, y, \lambda, p) \\ g(x, y, \lambda, p) \end{bmatrix} = F(z, \lambda, p) = 0 \quad (2)$$

And  $D_z F|_0$  has a zero eigenvalue (or zero singular value) [12]. This equilibrium is typically associated to a saddle-node bifurcation point [10].

For a given set of controllable parameters  $p_0$ , voltage collapse studies usually concentrate on determining the collapse or bifurcation point  $(x_0, y_0, \lambda_0)$ , where  $\lambda_0$  typically corresponds to the maximum loading level or loadability margin in p.u., %, MW, Mvar or MVA, depending on how the load variations are modeled and defined. Based on bifurcation theory, two basic tools are typically applied to the computation of the collapse point, namely, direct and continuation methods.

In voltage collapse studies, the continuation method shows many advantages, so, most of the reaserchers apply this technique to trace voltage profile at various buses of the test power system, with respect to changes of loading level  $\lambda$ , namely, Continuation Power Flow (CPF).

In this paper the continuation power flow algorithm with smooth changes of loading level at various buses of the system, is chosen for simulation purpose.

## III. CONTINUATION POWER FLOW (CPFLOW)

Continuation methods are typically used to determine the proximity to saddle node bifurcations in dynamic systems. Continuation power flows trace the solution of the power flow equation  $s(z, \lambda) = 0$ , where the parameter  $\lambda$  stands for the loading factor. The method can be summarized in two steps: [4].

### A. PREDICTOR STEP

At a generic equilibrium point  $p$ , the following relation applies:

$$\begin{aligned} f(x_p, \lambda_p) = 0 &\Rightarrow \left. \frac{df}{d\lambda} \right|_p = 0 \\ \Rightarrow D_x f|_p \left. \frac{dx}{d\lambda} \right|_p + \left. \frac{\partial f}{\partial \lambda} \right|_p &= 0 \end{aligned} \quad (3)$$

and the tangent vector can be approximated by:

$$\tau_p = \left. \frac{dx}{d\lambda} \right|_p \approx \frac{\Delta x_p}{\Delta \lambda_p} \quad (4)$$

From (5) and (6)

$$\tau_p = -D_x f|_p^{-1} \frac{\partial f}{\partial \lambda} \Big|_p \quad (5)$$

$$\Delta x_p = \tau_p \Delta \lambda_p$$

At this point a step size control  $k$  has to be chosen in order to determine the increment  $\Delta x_p$  and  $\Delta \lambda_p$ , along with a normalization to avoid large steps when  $\|\tau_p\|$  is large

$$\Delta \lambda_p = \frac{\Delta}{\|\tau_p\|} k \quad \Delta x_p = \frac{\Delta}{\|\tau_p\|} k \tau_p \quad (6)$$

where  $\|\cdot\|$  is the Euclidean norm and  $k = \pm 1$ . The sign of  $k$  determines the increase or the decrease of  $\lambda$ .

Figure 1 presents a pictorial representation of the predictor step.

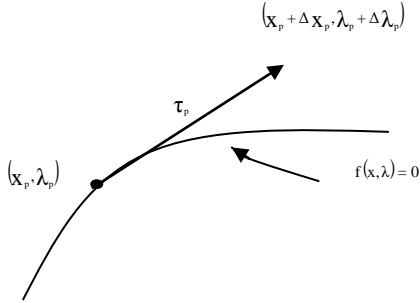


Fig. 1. Continuation Power flow: predictor step obtained by means of tangent

### B. CORRECTOR STEP

In the corrector step, a set of  $n+1$  equations is solved:

$$f(x, \lambda) = 0$$

$$\eta(x, \lambda) = 0$$

Where the solution of  $f(x, \lambda) = 0$  must be in the bifurcation manifold and  $\eta(x, \lambda) = 0$  is an additional equation to guarantee a non singular set at the bifurcation point.

For the choice of  $\eta$  there are two options: the perpendicular intersection  $\eta$  and the local parameterization.

In case of perpendicular intersection, whose pictorial representation is depicted in figure 2, the expression of  $\eta$  becomes:

$$\eta(x, \lambda) = \begin{bmatrix} \Delta x_p \\ \Delta \lambda_p \end{bmatrix}^T \begin{bmatrix} x_c - (x_p + \Delta x_p) \\ \lambda_c - (\lambda_p + \Delta \lambda_p) \end{bmatrix} = 0 \quad (7)$$

Whereas for the local parameterization, either the parameter  $\lambda$  or a variable  $x_i$  is forced to be a fixed value

Or

$$\eta(x, \lambda) = \lambda_c - \lambda_p - \Delta \lambda_p$$

$$\eta(x, \lambda) = x_{ci} - x_{pi} - \Delta x_{pi} \quad (8)$$

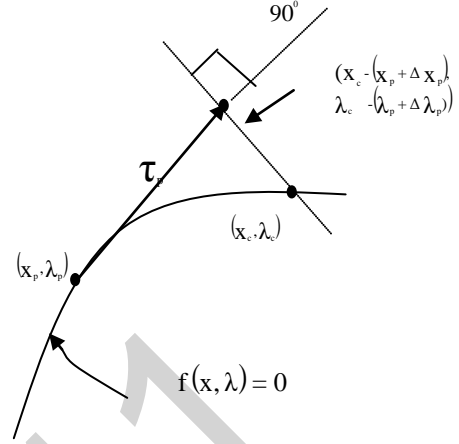


Fig. 2. Continuation Power flow: corrector step obtained by means of perpendicular intersection.

The choice of the variable to be fixed depends on the bifurcation manifold of  $f$ , as depicted in figure 3.

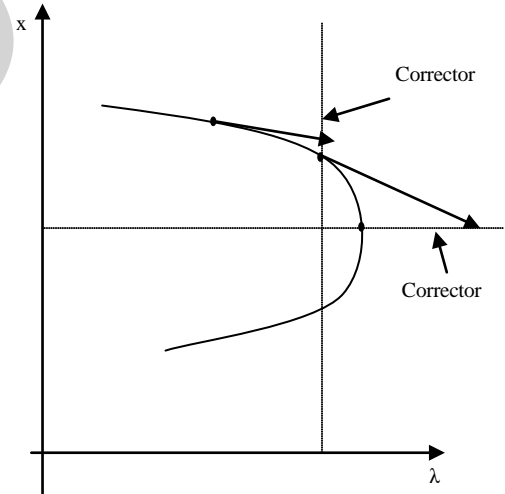


Fig. 3. Continuation Power flow: corrector step obtained by means of local parameterization

## IV. FACTS MODELING

Each model is described by a set of differential algebraic equations :

$$\dot{x}_c = f(x_c, x_s, V, \theta, u)$$

$$\dot{x}_s = f(x_c, x_s, V, \theta)$$

$$P = g_p(x_c, x_s, V, \theta) \quad (9)$$

$$Q = g_p(x_c, x_s, V, \theta)$$

Where:

$x_c$  is the control system variable,

$x_s$  is the controlled state variable (e.g firing angle)

$V$  and  $\theta$  are the voltage amplitude and phases at the buses at which the components are connected.

$u$  represents the input control parameters, such as reference power flows. FACTS models are based on what was proposed in [11].

### A. STATIC VAR COMPENSATION (SVC)

The two most popular configuration of this type of shunt controller are the fixed capacitor (FC) with a thyristor controlled reactor (TCR) and the thyristor switched capacitor (TSC) with TCR. Among these two setups, the second (TSC-TCR) minimizes stand-by losses; however from a steady-state point of view, this is equivalent to the FC-TCR. In this paper, the FC-TCR structure is used for analysis of SVC which is shown in figure 4.

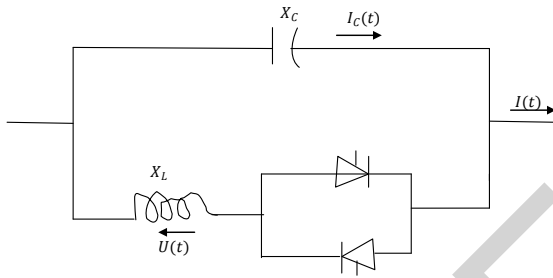


Fig. 4 Equivalent FC-TCR circuit of SVC

The TCR consists of a fixed reactor of inductance  $L$  and a bi-directional thyristor valve that are fired symmetrically in an angle control range of  $90^\circ$  to  $180^\circ$ , with respect to the SVC voltage.

Assuming controller voltage equal to the bus voltage and performing a Fourier series analysis on the inductor current wave form, the TCR at fundamental frequency can be considered to act like variable inductance given by [7]:

$$X_V = X_L \frac{\pi}{2(\pi - \alpha) + \sin 2\alpha} \quad (10)$$

Where,  $X_L$  is the reactance caused by the fundamental frequency without thyristor control and  $\alpha$  is the firing angle.

Hence, the total equivalent impedance of the controller can be represented as:

$$X_e = X_c \frac{\pi/r_x}{\sin 2\alpha - 2\alpha + \pi(2 - 1/r_x)} \quad (11)$$

Where  $r_x = X_C/X_L$ . The limits of the controller are given by the firing angle limits, which are fixed by design. The typical steady-state control law of a SVC used here is depicted in figure 5, and may be represented by the following voltage-current characteristic:

$$V = V_{ref} + X_{SL} I \quad (12)$$

Where  $V$  and  $I$  stand for the total controller RMS voltage and current magnitudes, respectively, and  $V_{ref}$  represent a reference voltage.

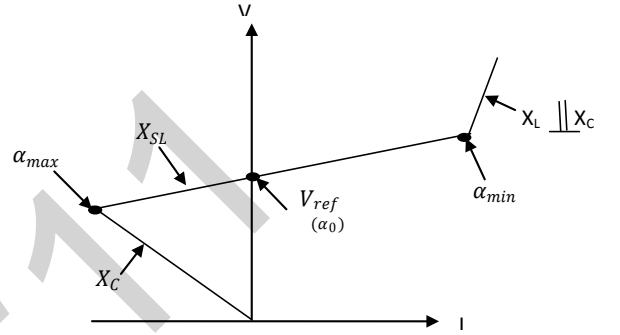


Fig. 5 Typical steady state V-I characteristic of a SVC

Typical values for the slope  $X_{SL}$  are in the range of 2 to 5 %, with respect to the SVC base; this is needed to avoid hitting limits for small variations of the bus voltage. A typical value for the controlled voltage range is  $\pm 5\%$  about  $V_{ref}$  [7]. At the firing angle limits, the SVC is transformed into a fixed reactance.

## V. SIMULATION RESULTS

A IEEE 14-bus test system as shown in figure 6 is used for voltage stability studies. The test system consists of five generators and eleven PQ bus (or load bus). The simulation was done using PSAT and MATLAB [12]. PSAT is a power system analysis software, which has many features including power flow and continuation power flow. Using continuation power flow feature of PSAT, voltage stability of the test system is investigated.

### A. LOCATION OF SVC

The behaviour of the test system with and without SVC under different loading conditions is studied.

The location of the SVC device is determined through CPFlow technique.

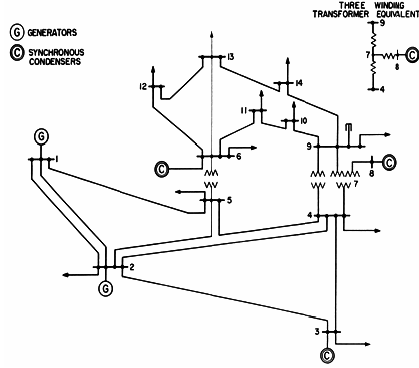


Fig. 6 The IEEE 14-bus test system

A typical PQ model is used for the loads and the generator limits are ignored.

Voltage stability analysis is performed by starting from an initial stable operating point and then increasing the loads by a factor  $\lambda$  until singular point of power flow linearization is reached. The loads are defined as

$$P_l = \lambda P_0$$

$$Q_l = \lambda Q_0$$

where  $P_0$  and  $Q_0$  are the active and reactive base loads, whereas  $P_l$  and  $Q_l$  are the active and reactive loads at bus 1 for the current operating point as defined by  $\lambda$ .

From the CPFlow analysis which are shown in the figure 7, the buses 4, 5, 9 and 14 are the critical buses.

Figure 8 shows PV curves for the critical buses for 14-bus test system without SVC.

Maximum loading point or bifurcation point where the Jacobian matrix becomes singular occurs at  $\lambda = 2.76$ , bus 14 is indicated as the critical voltage bus needing Q support.

Whereas figure 9 shows the P-V curves at bus 14 for different contingencies for the IEEE 14-bus test system.

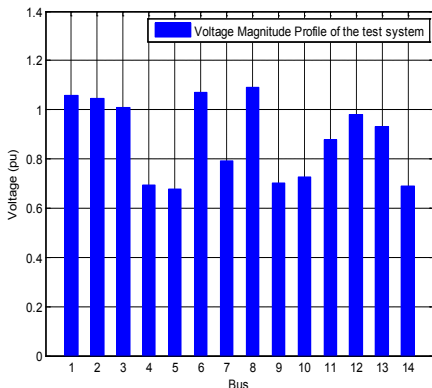


Fig. 7 Voltage Profile of IEEE 14 Bus system

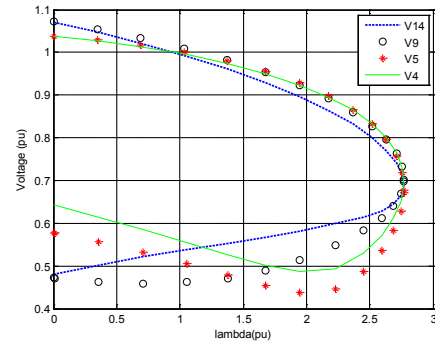


Fig. 8 PV curve for 14 bus system without SVC

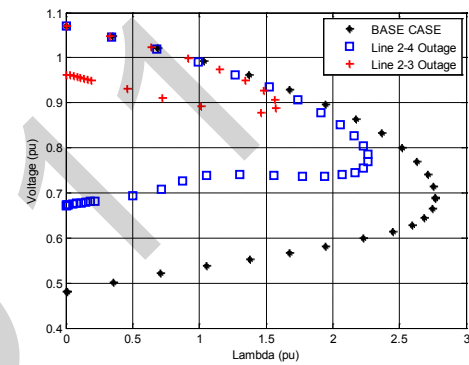


Fig. 9 PV curve at bus 14 for different contingencies

## B. DESIGN OF SVC

After the optimal location of the SVC was determined to be at bus 14, the ratings of the SVC have to be chosen. It is to be expected that by introducing a SVC at that location. The voltage profiles will be flatter and the loadability margin of the system will increase. Assuming a typical control range for the voltage at that bus, i.e.,  $\pm 5\%$ , one can treat that bus as a PV bus with the voltage fixed at 0.95 p.u. This means placing a reactive power source, i.e.; a synchronous compensator, at that bus. Considering that the SVC has to control the voltage at the loading level where the system without the SVC collapses, the required reactive power injection at that bus is found from the power flow. This is the maximum capacitive rating of the SVC. If the inductive power rating of the SVC is considered equal to the capacitive rating at 1.05 p.u. bus voltage, then the inductive reactance  $X_L$  of the SVC is 55% of the capacitive reactance  $X_C$  [11].

## C. PV curve for the system

The voltage profiles for the system with the SVC at bus 14 are shown in figure 10. As expected, the bifurcation for the system with the SVC placed at bus 14 occurs at a higher load value, i.e.,  $\lambda = 2.85$ .

Also, the voltage profiles are much flatter within the control limits of the SVC. Which are reached by design at

approximately the previous bifurcation value  $\lambda = 2.76$ .

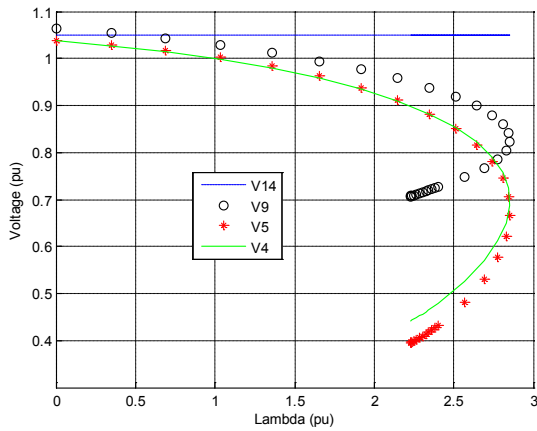


Fig. 10 PV curve for 14 bus system with SVC at bus 14

Voltages profiles of base case and system with SVC are illustrated in figure 11. It is obviously from figure 11 SVC provides a better voltage profile at the collapse point. This is due to the reason that the SVC is installed at the weakest bus.

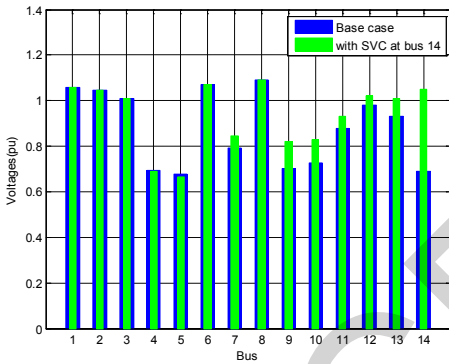


Fig. 11. Voltage Profile of system with SVC

The nose curves for the system with the same SVC located now at bus 9 are shown in figure 12. The controlled range of the voltages is considerably less than for the SVC placed at bus 14. Furthermore, the bifurcation occurs at a lower load value of  $\lambda = 2.82$ .

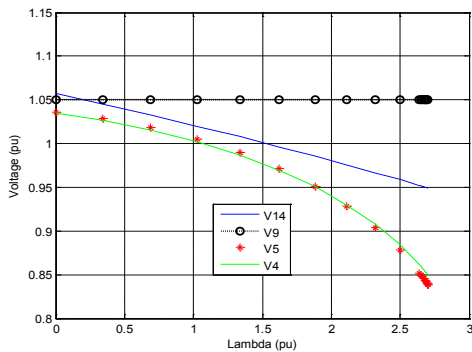


Fig. 12 PV curve for 14 bus system with SVC at bus 9

#### D. Voltages Profiles for line 2-3 outage

Voltages profiles at the collapse point for line 2-3 outage and system with SVC are illustrated in figure 13. From figure 13, SVC provides a better voltage profile at the collapse point.

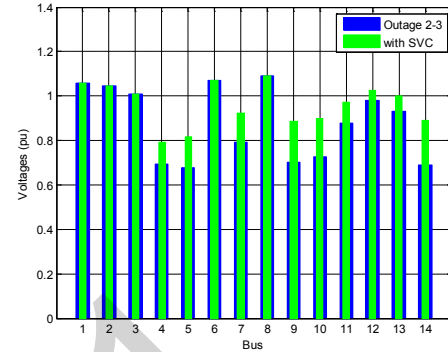


Fig. 13 Voltage Profile of line 2-3 outage with SVC

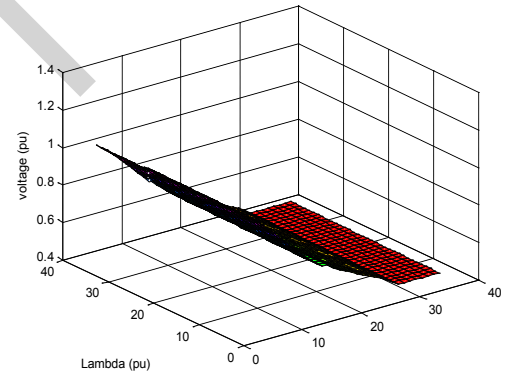


Fig.14. PV surface for bus number 14 of 14-bus test system without SVC

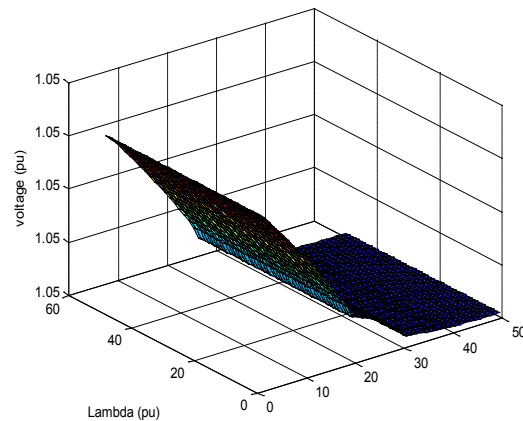


Fig. 15. PV surface for bus number 14 of 14-bus test system

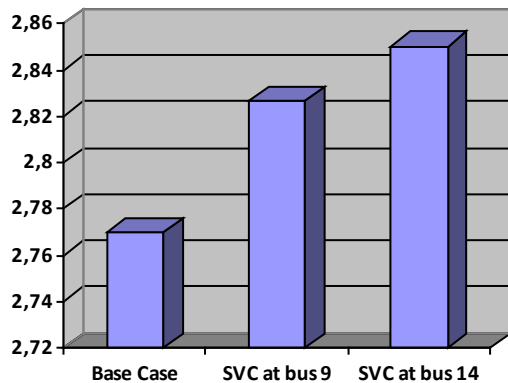


Fig. 16. Maximum loading point with SVC device

## VI. CONCLUSION

The results presented in this paper clearly show how SVC can be used to increase system loadability in practical power system. The test system requires reactive power the most at the weakest bus, which is located in the distribution level. Introducing reactive power at this bus using SVC can improve loading margin the most. In this paper adequate models for the SVC in the steady state studies are presented and thoroughly discussed. Hence, a technique to identify the optimal placement of the SVC device and related equations are derived. The results of simulations on the IEEE 14 bus test system have clearly shown that how SVC device increased the buses voltage, power limits, line powers, and loading capability of the network.

## APPENDIX

PV surface of buse 14 of the IEEE 14- bus test system is without and with SVC shown in figures 14-15.

From figure 16 it is obviously that the loading parameter of the system with SVC at bus 14 is highest while that without SVC is lowest.

## ACKNOWLEDGMENT

The authors would like to acknowledge the financial support of the M.E.S.R.S, Algeria, under project: J2001/02/52/05.

## REFERENCES

- [1] Repo, S.: On –Line voltage stability assessment of power System-An Approach of Black-box modelling. Tampere University Of technology publications 344, Tampere, 2001.
- [2] Yome, A.S.- Mithulananthan, N – Lee, K, Y.: Static Voltage Stability Margin Enhancement using STATCOM, TCSC and SSSC. IEEE/PES Transmission and Distribution conference and Exhibition, Asia and Pacific, DalianChina, 2005.

- [3] Blackout of 2003: Description and Responses, Available: <http://www.pserc.wisc.edu/>.
- [4] Natesan, R.- Radman, G.: Effects of STATCOM, SSSC and UPFC on Voltage Stability. Proceeding of the system theory, thirty-Sixth southeastern symposium, 2004, pp.546-550.
- [5] Dobson.- Dchiang, H.: Towards a theory of Voltage collapse in electric power systems. Systems and Control Letters, Vol.13,1989, pp.253-262.
- [6] Canizares, C.A.- Alarado, F.L.- DeMarco, C.L.- Dobson, I.- Long, W.F.: Point of collapse methods applied to ac/dc power systems. IEEE Trans. Power Systems, ol.7, n° 2, May 1992, pp.673-683.
- [7] Canizares, C.A.- Faur, Z. “ Analysis of SVC and TCSC controllers in voltage collapse. IEEE Trans. On Power systems, vol. 14, No. 1, pp. 158-165, Feb. 1999.
- [8] Kazemi, A.- Vahidinasab, V.- Mosallanejad, A.: Study of STATCOM and UPFC controllers for Voltage Stability Evaluated by Saddle-Node Bifurcation Analysis. First International Power and Energy Conference PECon/IEEE, Putrajaya Malaysia, Novembre 28-29, 2006.
- [9] Talebi, N.- Ehsan, M. - Bathaee, S, M, T.: Effects of SVC and TCSC Control Strategies on Static Voltage Collapse Phenomen. IEEE Proceedings, SoutheastCon, pp.161-168, Mar 2004.
- [10] Canizares, C.A.: Power Row and Transient Stability Models of FACTS controllers for Voltage and Angle Stability Studies. IEEE/PES WM Panel on Modeling, Simulation and Applications of FACTS Controllers in Angle and Voltage Stability Studies, Singapore, Jan 2000
- [11] Zeno, T, Faur.: Effects Of Facts Devices On System loadability. Proc. North American Power Symposium, Bozeman, Montana, October 1995.
- [12] Milano, F.: Power System Analysis Toolbox, Version 2.0.0.-b2.1, Software and Documentation” February 14, 2008.

**Oum El F adhel Loubaba Bekri** : was born in Saida, Algeria, received her Bachelor (1986) and Eng. degree in Electrical Engineering from Sidi Bel-Abbes University in Algeria (1992), and her Master from ENSET, Oran, Algeria (2002). She worked in University Dr Moulay Tahar, Saida, Algeria from 1992 to 2010. She is currently a member of the Intelligent Control and Electrical Power Systems Laboratory, Djillali Liabès University, Sidi Bel Abbès, Algeria. Her current research interest includes Power Systems and FACTS.

**Mohammed-Karim Fellah**: was born in Oran, Algeria, in 1963. He received the Eng. degree in Electrical Engineering from University of Sciences and Technology, Oran, Algeria, in 1986, and The Ph.D. degree from National Polytechnic Institute of Lorraine (Nancy, France) in 1991. Since 1992, he is Professor at Djillali Liabès University of Sidi-bel-Abbès (Algeria). Between 2000 and 2010, he was Director of the Intelligent Control and Electrical Power Systems Laboratory at this University. His current research interest includes Power Electronics, HVDC links, and Drives.

**Mohamed-Fouad Benkhoris** was born in Bou-sâada, Algeria, on September 17, 1963. He has studied at Ecole Nationale Polytechnique d’Alger (ENPA), Algeria, and received the Engineer degree in electrical engineering (1986). In 1991 he obtained his PHD degree in electrical engineering at INP Lorraine (France). From 1991, he is an Assistant Professor at the Department of Electrical Engineering, of Polytech’Nantes, France. Since 2006 he is Professor at Polytech’Nantes, France. He makes research activities at the laboratory :

“Institut de Recherche en Electronique et Electrotechnique de Nantes Atlantique”(IREENA) Saint Nazaire, France.

His fields of interest are: dynamical modelling, simulation and control of electrical drives and especially multi phase drive, multi-converters systems and embarked network.

ICEO'11